

High Resolution Atomic Force Microscopy Imaging of Nucleic Acids

Pablo Ares¹, Julio Gomez-Herrero^{1,3}, and Fernando Moreno-Herrero^{*2}

¹ Department of Condensed Matter Physics. Universidad Autónoma de Madrid. E-28049 Madrid, Spain.

² Department of Macromolecular Structures, Centro Nacional de Biotecnología, Consejo Superior de Investigaciones Científicas, 28049 Cantoblanco, Madrid, Spain.

³ Condensed Matter Physics Center (IFIMAC), Universidad Autónoma de Madrid, E-28049, Madrid, Spain.

*Corresponding Author. E-mail: fernando.moreno@cnb.csic.es.

Abstract.

Exploring the limits of spatial resolution has been a constant in history of Atomic Force Microscopy imaging. Since its invention in 1986, the AFM has beaten the barrier of resolution continuously thanks to technical developments, miniaturization of tips and implementation of new imaging modes. The double-helix structure of DNA has been always at the horizon of resolution. Today, this milestone has been reached, not only imaging DNA, but also its close relative double-stranded RNA. Here we provide a comprehensive description of the methods employed and the steps required to image the helical periodicity of these two nucleic acids with the sample immersed in a buffer solution.

Running title: AFM of nucleic acids

Keywords.

Atomic Force Microscopy, double-stranded DNA, double-stranded RNA, AFM imaging methods

1. Introduction.

In Atomic Force Microscopy, a sharp tip supported by a micrometer-size cantilever is employed to scan and probe the topography of a surface. Tip-sample interaction is transduced into a change of a parameter of the supporting cantilever (typically deflection, oscillation amplitude or frequency), which is used as control in a feedback loop to obtain a topographic image. The high sensitivity of the technique in the vertical dimension relies on the strong dependence of the tip-sample interaction with the tip-sample distance. However, the lateral resolution of AFM has been always punished by the finite size of the tip giving rise to the so-called tip-dilation problem when imaging objects smaller than the size of the tip. The development of new imaging modes and most importantly, the use of cantilevers with resonance frequency of tens of kHz in liquid and low stiffness, have been critical to improve the level of control on the tip-sample distance and, consequently, on the force applied to soft materials such as nucleic acids [1-3]. Since high imaging speed is not a requirement here, cantilevers do not need to be ultra-small and regular commercial cantilevers available for most AFM setups are valid for high resolution. Nevertheless, in principle high-speed imaging may be beneficial to improve spatial resolution as low frequency noise effects are reduced. Minimization of the force exerted by the tip has proven to be fundamental to achieve high resolution of soft matter, but still in order to probe narrow and deep trenches a sharp tip is required. We have found that the combination of small forces and sharp point tips are the key factors to image with enough resolution to resolve the helical structure of nucleic acids. On the contrary, the imaging mode chosen to scan the sample was not critical.

Despite the seminal work by Mou et al. [4] in contact mode, it has been only recently when the double helix of DNA has been clearly resolved using dynamic modes [5-7,1,2]. High resolution AFM imaging of double stranded RNA has also been recently reported [3]. The more commonly used AFM dynamic modes are Amplitude Modulation AFM (AM-AFM, also known as Tapping or

intermittent contact) [8,9] and Frequency Modulation AFM (FM-AFM) [10-13]. Other advanced dynamic modes include Drive Amplitude Modulation (DAM-AFM) [14], Kelvin Probe Force Microscopy [15], and multi-frequency based imaging modes [16]. In dynamic modes the cantilever is oscillated at or near its resonance frequency and either the cantilever oscillation amplitude (AM-AFM) or the frequency shift (FM-AFM) are used as control parameter for topographic imaging. Force-distance based imaging modes include PeakForce Tapping [17] or Jumping Mode plus (JM+) [18-20]. These imaging modes use the force given by the deflection of the cantilever as control parameter. In references [2] and [3] it is also proved that force-distance based imaging modes can be used for high resolution imaging of nucleic acids.

A list of requirements for high resolution imaging is given below.

A soft tip sample-interaction. In dynamic modes, this is achieved using cantilevers with a high resonance frequency (e.g. ~ 110 kHz in air conditions, typically 25 kHz in liquid) and a low constant force (e.g. ~ 0.09 N m⁻¹), and this necessarily requires relatively small cantilevers. In force-distance based modes the cantilever is not driven at its resonance frequency. However, in order to minimize drag forces, which result in a hysteresis deflection loop, small cantilevers are also desirable. Fine tuning of parameters for each imaging mode is essential (see below).

Sharp tips. Most commercially available AFM tips have a nominal radius (< 10 nm) larger than the size of a nucleic acid groove. However, this showed not to be essential to resolve the helical periodicity of dsDNA [2] and dsRNA [3]. A plausible explanation is that the small features of the biological specimens are probed by a tiny irregularity at the end of the tip, which effectively is able to get insight the grooves. Note, however that probing at the grooves is possible only if low forces are maintained while imaging. This also introduces a random factor in the experiments: not all cantilevers perform the same in terms of high resolution.

Minimization of cantilever spurious resonance peaks in liquid. In dynamic modes, the cantilever is oscillated at or near its resonance frequency. Due to the low quality factor of the cantilever

resonance in liquids, its response in these media is broad and acoustic excitation of the tip holder can produce multiple spurious peaks. Not all of these peaks, which could hide the real one, work satisfactorily for dynamic modes operation. For high resolution imaging it is important to have a clean resonance peak. Different AFM designs deal with this problem using different strategies, which include photothermal [21] and magnetic excitation [22] of the tip, or optimized acoustic excitation [23].

High sensitivity of the detection system. The relation between the distance the cantilever moves (in nanometers) and the output it generates at the detection system (in Volts) is known as the deflection sensitivity (in nm V^{-1}). A low value of this magnitude ($< 20 \text{ nm V}^{-1}$) has proven to be crucial to control the low amplitudes and forces required for high resolution imaging.

High mechanical and thermal stability. The microscope has to be stable over image acquisition. These systems are often inside an acoustic isolation enclosure placed over an active or passive vibration isolation system. An RMS noise in vertical direction lower than $\sim 0.5 \text{ \AA}$ must be achieved. Regarding thermal stability, it is desirable to keep the microscope in a constant temperature environment to minimize thermal tip-sample drift. Low temperatures ($15\text{-}18^\circ\text{C}$) will also reduce liquid evaporation and changes in buffer composition. Rotation of the image scan area to make DNA/RNA molecules to coincide with the fast scanning direction also minimizes drift effects (see below).

Precise scanner calibration and low electronic noise. AFM piezo scanners are factory calibrated to adapt the piezo driving voltages to the required scanning sizes. The specifications of the scanner should be appropriate for high resolution imaging (noises must be lower than 1 \AA in the XY directions and 0.5 \AA in the Z direction). Additionally, for high resolution measurements it is advisable to recalibrate the piezo scanner using AFM test grids with pitch distances as close as possible to the distances to be measured. Otherwise the helical features of the nucleic acids might be imaged at wrong sizes. For instance, atomic steps (0.34 nm) in a graphite surface can

be used to accurately calibrate along the vertical direction, and its atomic periodicity (0.25 nm) to calibrate along the X-Y directions.

2. Materials

1. Cantilevers: Biolever mini BL-AC40TS-C2 available from Olympus.
2. V-4 grade mica sheets (SPI supplies). Mica substrates are fixed with double side tape to magnetic AFM specimen discs of 15 mm diameter (Ted Pella, INC).
3. Plasmid pGEM3Z (Promega) at 1 $\mu\text{g}/\mu\text{l}$.
4. Restriction enzyme BamHI (New England Biolabs).
5. RNase free DNase I (Roche).
6. QIAquick PCR purification Kit (Qiagen).
7. RNeasy MinElute Cleanup Kit (Qiagen).
8. HiScribe T7 *in vitro* Transcription Kit (New England Biolabs).
9. Chemicals to prepare buffers: NiCl_2 , Tris base, and HCl to adjust the pH to 8.0.
10. MilliQ-quality water.
11. Buffer A: 10 mM NiCl_2 , 10 mM Tris-HCl pH 8.0.
12. Buffer B: 10 mM Tris-HCl pH 8.0.
13. Double-stranded DNA and RNA molecules produced following the methods described below and stored in TE buffer at 4°C at a concentration of $\sim 0.6 \text{ ng}/\mu\text{l}$.
14. Atomic Force Microscope instrument from Nanotec Electronica S.L.

3. Methods

3.1 Fabrication of dsDNA molecules for high-resolution AFM imaging

dsDNA molecules in their linear form are typically produced by PCR or restriction digestion of plasmids that contain sites of interest or particular structures. Multiple DNA plasmids are commercially available but can be also produced by cloning in bacteria. DNA molecules

produced from plasmid restriction are often more homogeneous in size than those fabricated by PCR.

1. Cleave the pGem3Z plasmid with BamHI, mix 1 μg of pGem3Z (1 μl from stock at 1 $\mu\text{g}/\mu\text{l}$) with 1 μl BamHI (stock at 20 units/ μl) in 1X NEBuffer 3.1 for a total volume of 20 μl and incubate the mixture for 1 hour at 37°C.
2. Purify the linearized DNA using the QIAquick PCR purification kit following the instructions of the manufacturer. DNA is eluted in 20 μl of TE buffer (10 mM Tris-HCl pH 8.0, 1 mM EDTA).
3. Measure the concentration of DNA and prepare a dilution of 0.6 ng/ μl for AFM measurements.

3.2 Fabrication of dsRNA molecules for high-resolution AFM imaging

dsRNA molecules are fabricated by annealing two complementary single-stranded RNA molecules produced by transcription using T7 RNA polymerase on an appropriate dsDNA template containing the T7 RNA polymerase promoter. After transcription and annealing, the dsRNA is purified by RNeasy MinElute Cleanup Kit (Qiagen) and stored in TE buffer [24] [25].

1. Fabricate complementary ssRNA strands by transcription. Transcription is performed at 42°C for 3h, in RNase free PCR tubes using the HiScribe T7 *in vitro* Transcription Kit, with 1500U of T7 RNA polymerase in a total reaction volume of 60 μl .
2. Anneal the complementary ssRNA strands. After 3h of transcription reaction, pause the reactions and add EDTA to reach a final concentration of 30 mM EDTA (10.6 μl of 0.2 M EDTA in 500mM Tris, pH 8.0, in RNase free water). Mix both transcription reactions to anneal the complementary ssRNA strands. Annealing is achieved by heating for 1h at 65°C and slowly cooling down to room temperature at 1.2°C/5 min rate. Resulting

dsRNA molecules are purified using the QiaGen RNeasy Purification Kit, and eluted in RNase free water.

3. Eliminate the template DNA by digestion with 5U of RNase free DNase I (Roche) for 1h at 37°C.
4. Purify the dsRNA molecules by using the QiaGen RNeasy MinElute Cleanup kit, eluting in RNase free water or TE buffer.
5. Measure the concentration of dsRNA and prepare a dilution of 0.6 ng/ μ l for AFM measurements.

3.3 dsDNA and dsRNA sample preparation for high-resolution AFM imaging

For imaging of nucleic acids, mica is the substrate of preference because it exposes a clean and atomically-flat surface after mechanical cleavage that can be recycled multiple times. Importantly, immediately after its cleavage, the mica surface is always negatively charged and this allows the use of different divalent cations to attach negatively charged molecules such as DNA and RNA. These include Mg^{2+} , Ca^{2+} , Mn^{2+} , and Ni^{2+} , which electrostatically bridge the negatively charged surface of mica with DNA or RNA. We found that a millimolar concentration of $NiCl_2$ was enough to firmly attach both dsDNA and dsRNA to the mica surface [25].

1. Functionalize the mica surface. First cleave the mica and then add 10 μ l of buffer A. Leave for 1 minute.
2. Add 1 μ l (0.6 ng) of dsDNA or dsRNA to the droplet and wait for up to 15 minutes. To avoid evaporation, the sample can be covered by small box and a beaker with water placed inside to increase the local humidity.
3. Add 40 μ l of buffer A and then add 50 μ l of buffer B to reach a final volume of 100 μ l.
4. Place the sample on the stage of the AFM (**3.4, step 9**).

3.4 AFM set up

Most of the AFMs use the optical beam deflection method to detect the deflection of the cantilever [26] due to its simplicity, reliability, low noise and its ability to be applied to a variety of cantilevers. Hence, we will only consider AFMs of this kind. The following steps 1-8 should be performed before or during sample preparation. Steps 9-14 should be applied after sample preparation.

1. Turn on the AFM control unit and run the acquisition software. This will allow the electronics of the AFM to warm up.
2. Insert a cantilever into the cantilever holder and place it into the AFM head.
3. Align the laser beam to be focused on the cantilever.
4. Adjust the photodiode position maximizing the total intensity of light.
5. Calibrate the cantilevers' spring constant. Thermal [27] and Sader's [28] methods are the commonest. If your AFM control software includes a calibration method, follow the manufacturer's instructions. Otherwise, you can use either thermal or Sader's method (see **Note 1**).
6. Switch on the AM-AFM mode and tune the cantilever resonance frequency.
7. Place a dummy mica substrate (with the same thickness of the substrate employed in the nucleic-acid specimen) into the sample holder and mount it on the AFM scanner.
8. Coarse approach the cantilever to the substrate until a distance of less than 1 mm between the cantilever chip and the mica is observed. Remove the AFM head from the

acquisition position. This will prevent from crashing the tip later when placing the AFM head on the DNA/RNA sample with liquid.

9. Load the sample (mica substrate + nucleic acids) onto the AFM scanner. Sample should be prepared just before loading into the AFM. Special care should be taken to prevent that sample gets dry.
10. Pre-wet the cantilever chip by placing a drop of $\sim 30 - 40 \mu\text{l}$ of buffer B directly on the cantilever holder (*see Note 2*). This volume may change depending on the cantilever-holder design.
11. Return the AFM head to its acquisition position.
12. Due to the presence of liquid, the position of the laser on the cantilever has moved in the longitudinal direction of the cantilever. Realign it.
13. Readjust the photodiode position.
14. Retune the cantilever resonance frequency. Due to the presence of liquid the new value should be $\sim 1/3 - 1/4$ of the value in air and the quality factor much lower.

3.5 Tip-sample approach

Independently of the acquisition mode, tip-sample approach is done in AM-AFM mode, since it is the easiest mode among the suitable ones for high resolution. Modern AFMs include easy-to-use routines for the tip-sample approach where no parameters selection is necessary. If this is not the case, follow the next steps.

1. Select a free oscillation amplitude relatively high, to a value of $\sim 7 - 10$ nm (see **Note 3**).
By using a value in this range, false engagements during approach in liquids will be minimized.
2. Select a set point value of about 75% of the free amplitude.
3. Select a value of about $15 \mu\text{m/s}$ for the approach speed.
4. Tip-sample approach routines typically use an approach control parameter (*i.e.*, amplitude reduction) to stop the motion. Select an initial conservative value.
5. Start the tip-sample approach motion. As the tip approaches the sample, the amplitude will decrease until reaching the approach control parameter condition.
6. If the approach motion stops quickly after motor movement, false engagement is occurring. If this happens, increase the value of the approach control parameter and start the approach procedure again. Repeat this step increasing the control parameter value until the tip engages the sample.
7. At this point, the amplitude equals the set point at 75% of the free amplitude, but since we are using low spring constant cantilevers, the tip might not be in imaging range. Change the set point, so the piezo scanner will carefully reduce the tip-sample gap, until the tip gets in imaging range (see **Note 4**).

3.6. Amplitude Modulation, AM-AFM mode

AM-AFM operates by using the amplitude of the cantilever oscillation as the control parameter for topography acquisition. A feedback diagram of this mode can be found in **Figure 1a**.

1. Once the tip is in imaging range, reduce the drive amplitude to about 1 nm, and the set point value accordingly to get back to imaging range (see **Note 5**). Keep a set point value just below the amplitude value at which the cantilever lifts off the sample, typically 0.5 – 0.8 nm. Using low oscillation amplitude is a key factor to obtain high resolution in liquid.
2. Select an area of $1 \times 1 \mu\text{m}^2$ with a resolution of 128×128 pixels and a scanning frequency of ~ 2 lines per s and start the scanning operation. A wide field is preferred at this moment to pinpoint molecules with straight segments over several tens of nm.
3. Reduce the scan sizes to $50 \times 50 - 150 \times 150 \text{ nm}^2$ and zoom in over straight DNA/RNA segments. Acquire at 512×512 pixels resolution and scanning frequencies of 3 – 5 lines per s. To visualize the helical features of the nucleic acids set the fast scan direction preferably parallel to the straight segments (see **Note 6**).
4. Initially scan each line in the image from left to right (trace direction) and from right to left (retrace direction). Then, if the topographic features are conserved in both trace and retrace images, you may acquire in trace direction only to double the scan rate.
5. In AM-AFM there is only one feedback loop where the amplitude is used as the controlled input for the topography feedback. Adjust the feedback gains to optimize topography acquisition (see **Note 7**).
6. If the effective tip radius is small enough, lower than ~ 2.5 nm according to [3], double stranded nucleic acids major and minor grooves should be visible. **Figure 1b** and **Figure 1c** shows examples of high-resolution images of dsDNA and dsRNA, respectively.

3.7 Drive Amplitude Modulation, DAM-AFM mode

DAM-AFM operates by using three different feedback loops. A Phase Lock Loop (PLL) is used to track the resonance frequency. A second feedback loop adjusts the drive amplitude in order to maintain the cantilever oscillation amplitude at a fixed value. The drive amplitude channel is related to the power dissipated by the tip-sample interaction. Finally, a third feedback loop controls the topography acquisition adjusting the position of the scanner in the z-direction by keeping the drive amplitude constant at a set point value. A feedback diagram of this mode can be found in **Figure 2a**.

1. Approach in AM-AFM mode (see section 3.6 above). Once the tip is in imaging range, withdraw the tip from the sample for about 1 μm . By doing this, we avoid any possible damage that may occur while performing the procedure to engage all the different feedback loops. One micrometer distance is also convenient to easily get back to imaging range.
2. Enable the PLL and adjust its feedback gains (see **Note 7**).
3. Enable an extra feedback loop. The input of this feedback is the cantilever amplitude and the output is the drive amplitude. Select a set point for this feedback of 0.5 - 0.8 nm. Adjust its feedback gains (see **Note 7**).
4. Change the topography feedback channel, selecting the drive amplitude as input channel. Check the numerical value of the drive amplitude and select a topography set point about 10% higher than this drive amplitude value.
5. Start the tip-sample approach motion as in **3.5, step 5**. As the tip approaches the sample, the drive amplitude will increase until reaching the drive amplitude set point. If it does not reach the region of tip-sample interaction (imaging range), increase the drive amplitude set point. As already mentioned, drive amplitude is related to the tip-sample

power dissipation. Typical values of drive amplitude set point for imaging nucleic acids are in the range of 0.2 - 0.5 fW (see **Note 8**).

6. Start image acquisition following the same steps as for AM-AFM mode (**3.6, steps 2 - 4**). Adjust the topography feedback gains, and readjust if necessary the other feedback gains to optimize topography acquisition (see **Note 7**).
7. Double stranded nucleic acids helical structure should be resolved. **Figure 2b** and **Figure 2c** show examples of dsDNA and dsRNA, respectively, where the helical pitch can be clearly resolved.

3.8 Force-distance based modes

Force-distance based modes operate by performing a quick FZ curve at each pixel of the scanned area. Depending on the AFM manufacturer, the name of the mode varies (Jumping Mode, Pulsed Mode, Peakforce Tapping®, QI™ mode, Force-distance mapping mode, HybriD™ Mode, etc.) and there are slight differences on the way the movement of the tip is performed. In this section we will consider Jumping mode plus (JM+) as it was described in reference [3]. JM+ moves the tip from pixel to pixel at the farthest tip-sample distance, thus minimizing lateral forces. JM+ uses the peak force referenced to the force baseline as the control parameter for the topography acquisition, allowing a precise direct control on the applied forces. A feedback diagram of this mode can be found in **Figure 3a**.

1. Once the tip is in imaging range (see approach in AM-AFM, section 3.6), remove the cantilever oscillation and select a low set point in contact mode. This will bring the tip to a gentle contact with the substrate (see **Note 9**).

2. Select the proper values for the Amplitude and Frequency of the Z excursion movement. Amplitudes of 15 - 35 nm and frequencies of 0.5 - 1 kHz should work fine for JM+ (see **Note 10**).
3. Select the option to compensate for the dragging force (if it is available at your AFM control software).
4. Select the set point with respect to the force baseline. Typical values for the force set point are of the order of 30 – 50 pN (see **Note 11**).
5. Start the image acquisition following the same steps as for AM-AFM mode (**3.6, steps 2 - 4**). In the case of JM+ the scan rate will be related to the Frequency of the Z excursion. The above mentioned parameters will give typical scan rates of 3 - 4 lines per s. Adjust the feedback gains to optimize topography acquisition (see **Note 7**).
6. Double stranded nucleic acids helical structure should be resolved. **Figure 3b** and **Figure 3c** show examples on dsDNA and dsRNA, respectively, where the helical pitch can be clearly resolved.

4. Notes

1. The “thermal method” is based on the cantilever’s thermal distribution spectrum (square of the fluctuations in amplitude as a function of frequency). According to the equipartition theorem, the mean-square amplitude of the cantilever’s thermal fluctuation in the vertical direction, $\langle z^2 \rangle$ can be expressed as $\langle z^2 \rangle = (k_B T)/k_N$, where k_B is Boltzmann’s constant, T is the temperature of the cantilever and k_N is the cantilever spring constant.

Sader’s method can be applied to rectangular cantilevers. It incorporates the viscosity and density of the medium in which the cantilever is immersed, along with experimentally determined values of the resonance frequency and quality factor, together with the length and

width of the cantilever. Thus it can be considered a geometric approach, although it does not need the cantilever thickness. The spring constant can be easily calculated online at the University of Melbourne webpage (<http://www.ampc.ms.unimelb.edu.au/afm/calibration.html>) or directly on some AFM control software.

2. Pre-wetting the cantilever is useful to preserve its integrity when forming a liquid meniscus between the cantilever holder and the sample. It is recommended to pre-wet the whole cantilever chip, as this will ensure a more stable liquid meniscus.

3. Some AFM systems display the cantilever amplitude in Volts. To convert the cantilever amplitude to nm, multiply the value in volts by the deflection sensitivity of the detection system, taking also into account possible gains that may be applied to the amplitude channel. For example, the typical sensitivity of our system is $\sim 10 \text{ nm V}^{-1}$, and therefore the approach amplitude of 10 nm corresponds to 1 V.

4. It might happen that the piezo scanner fully-extends before reaching the imaging position. If this happens, perform a coarse approach using motor steps until the vertical scanner position is within its elongation range. Change again the set point to extend the piezo until the tip gets in imaging range or repeat the coarse approach procedure. One way to check if the AFM is in imaging range is by performing a Force vs. Distance (FZ) curve, monitoring the Amplitude as the tip moves away from the sample. If the tip is in imaging range, the Amplitude should increase with tip-sample distance as far as the tip-sample interaction is relevant. Beyond this point the Amplitude remains constant.

5. To reduce the oscillation of the cantilever, first reduce the drive amplitude and then change the set point to drive the system back to imaging range. The cantilever oscillation is typically proportional to the drive amplitude. For example, a decrease of the drive amplitude by a factor of 10, implies an equivalent change of set point.

6. All scanning microscopies suffer from the so-called 1/f noise (being f the noise frequency). Thus low frequency signals contribute with high noise amplitudes. The 1/f noise mainly includes contributions from thermal drift and mechanical noise. AFM is an scanning technique where the tip is moved along to orthogonal directions. In general the fast scan direction is about two orders of magnitude faster than the other orthogonal direction. A common way to minimize the 1/f noise is to increase the acquisition frequency and this is easily done by measuring along the fast scan axis. By setting the fast scan direction to be parallel to the straight segments of the molecules, low frequency noise is minimized. Note that if the molecule is not aligned with the fast axis, points in close proximity will be probed within a long lag time contributing to 1/f noise that may result in loss of spatial resolution. Therefore, low frequency noise is much likely to have an effect on data points acquired along the slow scan direction and this is the reason why we rotate the image to have the molecules preferably aligned with fast scan axis (the horizontal axis of the image). Nevertheless, under conditions of very low thermal drift and mechanical noise, it is possible to observe the periodicity along molecules not aligned to the horizontal direction of the image [3].

7. The feedback gain values that optimize the acquisition without damaging the sample need to be determined for each AFM set up. In general, the higher the gain the faster will be the response. However, a too high gain value will produce instabilities and oscillations in the feedback.

8. The drive amplitude (in Volts) can be related to the power (Watts) dissipated between tip and sample. To convert Volts into Watts the Cleveland formula can be used [29]:

$$\overline{P_{tip}} = 2\pi f_0 \frac{1/2 kA^2}{Q} \left(\frac{V_{drive}}{V_{drive,0}} - \frac{f}{f_0} \right)$$

Where P_{tip} is the dissipation power, f_0 is the resonance frequency of the free cantilever, f is the resonance frequency in imaging range, k is its spring constant, A is its amplitude, Q is its quality

factor, $V_{drive,0}$ is the driving voltage applied to the free cantilever and V_{drive} is the driving voltage of the cantilever in imaging range.

9. When changing from AM-AFM to contact mode, check the value of the normal force before removing the cantilever oscillation and use a slightly higher value for the topography set point to establish a very gentle contact.

10. In JM+, the amplitude of the Z excursion is called Jump off, which typically ranges from 15 to 35 nm for this kind of experiments. The frequency of the Z excursion is controlled through two parameters, Jump sample and Control cycles. Values of 15 - 30 and 5 - 10, respectively, will provide a frequency of the Z excursion in the 0.5 - 1 kHz range. In JM+ the frequency of the Z excursion coincides with the frequency of pixel acquisition. Images of 256×256 pixels obtained by scanning only in the trace direction are typically taken in 120 seconds. Other force-based modes may operate using different frequencies.

11. These forces correspond to set points of 0.02 - 0.07 V, for Olympus Biolever mini cantilevers, and considering a deflection sensitivity of $< 20 \text{ nm V}^{-1}$.

In summary, high-resolution imaging of nucleic acids can be achieved by different imaging modes, provided the list of requirements given in the introduction is fulfilled. Therefore, the choice of a particular one should not be motivated by its resolution to image DNA or RNA, but by the additional information of the sample that each particular mode may provide. For instance, AM-AFM can give information on material composition via the phase/frequency shift channel, DAM-AFM allows the quantification of the power dissipated in the process of imaging; and force-distance based imaging modes give information on the mechanical properties of the sample.

Acknowledgments

We thank E. Herrero-Galan and C. Aicart for providing details of the protocol for dsRNA and dsDNA fabrication; and A. Gil for critical reading of the manuscript. We thank the financial support from the Spanish MINECO (projects MAT2016-77608-C3-3-P and The “María de Maeztu” Programme for Units of Excellence in R&D (MDM-2014-0377) to J.G.-H.; and FIS2014-58328-P to F.M.-H.). F.M.-H. also acknowledges support from European Research Council (ERC) under the European Union’s Horizon 2020 research and innovation (grant agreement No 681299).

References

1. Ido S, Kimura K, Oyabu N, Kobayashi K, Tsukada M, Matsushige K, Yamada H (2013) Beyond the helix pitch: direct visualization of native DNA in aqueous solution. *ACS Nano* 7 (2):1817-1822. doi:10.1021/nn400071n
2. Pyne A, Thompson R, Leung C, Roy D, Hoogenboom BW (2014) Single-molecule reconstruction of oligonucleotide secondary structure by atomic force microscopy. *Small* 10 (16):3257-3261. doi:10.1002/smll.201400265
3. Ares P, Fuentes-Perez ME, Herrero-Galan E, Valpuesta JM, Gil A, Gomez-Herrero J, Moreno-Herrero F (2016) High resolution atomic force microscopy of double-stranded RNA. *Nanoscale* 8 (23):11818-11826. doi:10.1039/c5nr07445b
4. Mou J, Czajkowsky DM, Zhang Y, Shao Z (1995) High-resolution atomic-force microscopy of DNA: the pitch of the double helix. *FEBS Lett* 371 (3):279-282
5. Maaloum M, Beker AF, Muller P (2011) Secondary structure of double-stranded DNA under stretching: elucidation of the stretched form. *Phys Rev E Stat Nonlin Soft Matter Phys* 83 (3 Pt 1):031903
6. Kitazawa M, Ito S, Yagi A, Sakay N, Uekusa Y, Ohta R, Inaba K, Hayashi A, Hayashi Y, Tanemura M (2011) High-Resolution Imaging of Plasmid DNA in Liquids in Dynamic Mode Atomic Force Microscopy Using a Carbon Nanofiber Tip. *Japanese Journal of Applied Physics* 50 (8):S3
7. Leung C, Bestembayeva A, Thorogate R, Stinson J, Pyne A, Marcovich C, Yang J, Drechsler U, Despont M, Jankowski T, Tschope M, Hoogenboom BW (2012) Atomic force microscopy with nanoscale cantilevers resolves different structural conformations of the DNA double helix. *Nano Lett* 12 (7):3846-3850. doi:10.1021/nl301857p
8. Lyubchenko YL, Shlyakhtenko LS (2009) AFM for analysis of structure and dynamics of DNA and protein-DNA complexes. *Methods* 47 (3):206-213. doi:S1046-2023(08)00150-3 [pii]

10.1016/j.ymeth.2008.09.002

9. Cassina V, Manghi M, Salerno D, Tempestini A, Iadarola V, Nardo L, Brioschi S, Mantegazza F (2015) Effects of cytosine methylation on DNA morphology: An atomic force microscopy study. *Biochim Biophys Acta*. doi:10.1016/j.bbagen.2015.10.006

10. Marti O, Drake B, Hansma PK (1987) Atomic force microscopy of liquid-covered surfaces: Atomic resolution images. *Appl Phys Lett* 51 (7):484-486

11. Martinez-Martin D, Carrasco C, Hernando-Perez M, de Pablo PJ, Gomez-Herrero J, Perez R, Mateu MG, Carrascosa JL, Kiracofe D, Melcher J, Raman A (2012) Resolving structure and mechanical properties at the nanoscale of viruses with frequency modulation atomic force microscopy. *PLoS One* 7 (1):e30204. doi:10.1371/journal.pone.0030204

12. Fukuma T, Jarvis SP (2006) Development of liquid-environment frequency modulation atomic force microscope with low noise deflection sensor for cantilevers of various dimensions. *Review of Scientific Instruments* 77:043701

13. Yamada H, Kobayashi K, Fukuma T, Hirata Y, T. K, Matsushige K (2009) Molecular resolution imaging of protein molecules in liquid using frequency modulation atomic force microscopy. *Applied Physics Express* 2 (9):095007

14. Jaafar M, Martinez-Martin D, Cuenca M, Melcher J, Raman A, Gomez-Herrero J (2012) Drive-amplitude-modulation atomic force microscopy: From vacuum to liquids. *Beilstein journal of nanotechnology* 3:336-344. doi:10.3762/bjnano.3.38

15. Nonnenmacher M, M.P. OB, Wickramasinghe HK (1991) Kelvin probe force microscopy. *Appl Phys Lett* 58 (25):2921-2923

16. Garcia R, Herruzo ET (2012) The emergence of multifrequency force microscopy. *Nat Nanotechnol* 7 (4):217-226. doi:10.1038/nnano.2012.38

17. Pittenger BB, Erina N (2012) Application Note #128. Quantitative Mechanical Property Mapping at the Nanoscale with PeakForce QNM. Bruker

18. de Pablo PJ, Colchero J, Gómez-Herrero J, Baro AM (1998) Jumping mode scanning force microscopy. *Appl Phys Lett* 73 (22):3300-3302

19. Ortega-Esteban A, Horcas I, Hernando-Perez M, Ares P, Perez-Berna AJ, San Martin C, Carrascosa JL, de Pablo PJ, Gomez-Herrero J (2012) Minimizing tip-sample forces in jumping mode atomic force microscopy in liquid. *Ultramicroscopy* 114:56-61. doi:10.1016/j.ultramic.2012.01.007

20. Rosa-Zeise A, Weilandt E, Hild S, Marti O (1997) The simultaneous measurement of elastic, electrostatic and adhesive properties by scanning force microscopy: pulsed-force mode operation. *Meas Sci Technol* 8:1333-1338

21. Kiracofe D, Kobayashi K, Labuda A, Raman A, Yamada H (2011) High efficiency laser photothermal excitation of microcantilever vibrations in air and liquids. *Rev Sci Instrum* 82 (1):013702. doi:10.1063/1.3518965

22. Han W, Lindsay SM, Jing T (1996) A magnetically driven oscillating probe microscope for operation in liquids. *Appl Phys Lett* 69 (26):4111-4113

23. Carrasco C, Ares P, de Pablo PJ, Gomez-Herrero J (2008) Cutting down the forest of peaks in acoustic dynamic atomic force microscopy in liquid. *Rev Sci Instrum* 79 (12):126106. doi:10.1063/1.3053369

24. Dekker NH, Abels JA, Veenhuizen PT, Bruinink MM, Dekker C (2004) Joining of long double-stranded RNA molecules through controlled overhangs. *Nucleic Acids Res* 32 (18):e140. doi:10.1093/nar/gnh138
25. Herrero-Galan E, Fuentes-Perez ME, Carrasco C, Valpuesta JM, Carrascosa JL, Moreno-Herrero F, Arias-Gonzalez JR (2013) Mechanical identities of RNA and DNA double helices unveiled at the single-molecule level. *J Am Chem Soc* 135 (1):122-131. doi:10.1021/ja3054755
26. Meyer G, Amer NM (1988) Novel optical approach to atomic force microscopy. *Applied Physics Letters* 53:1045
27. Butt H-J, Jaschke M (1995) Calculation of thermal noise in atomic force microscopy. *Nanotechnology* 6:1-7
28. Sader JE (1998) Frequency response of cantilever beams immersed in viscous fluids with applications to the atomic force microscope. *Journal of Applied Physics* 84:64
29. Cleveland JP, Anczykowski B, Schmid AE, Elings VB (1998) Energy dissipation in tapping-mode atomic force microscopy. *Appl Phys Lett* 72 (20):2613-1615

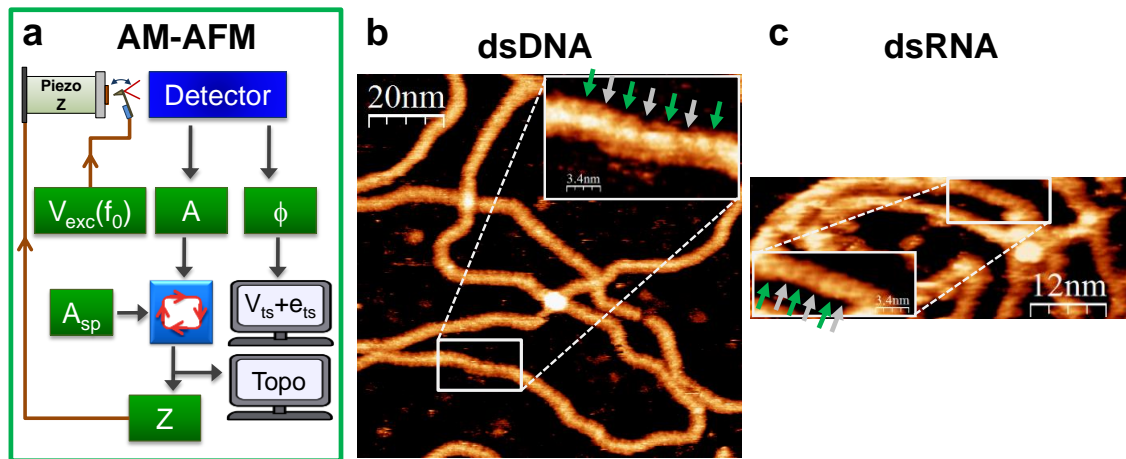


Figure 1. Amplitude Modulation AFM mode and high-resolution imaging of dsDNA and dsRNA.

a) Diagram of AM-AFM mode experimental setup. b) AM-AFM high-resolution image of dsDNA.

c) AM-AFM high-resolution image of dsRNA. Insets show fragments of dsDNA and dsRNA

molecules, where their major and minor grooves are resolved. Panels a and c, [3] - Adapted with

permission of The Royal Society of Chemistry.

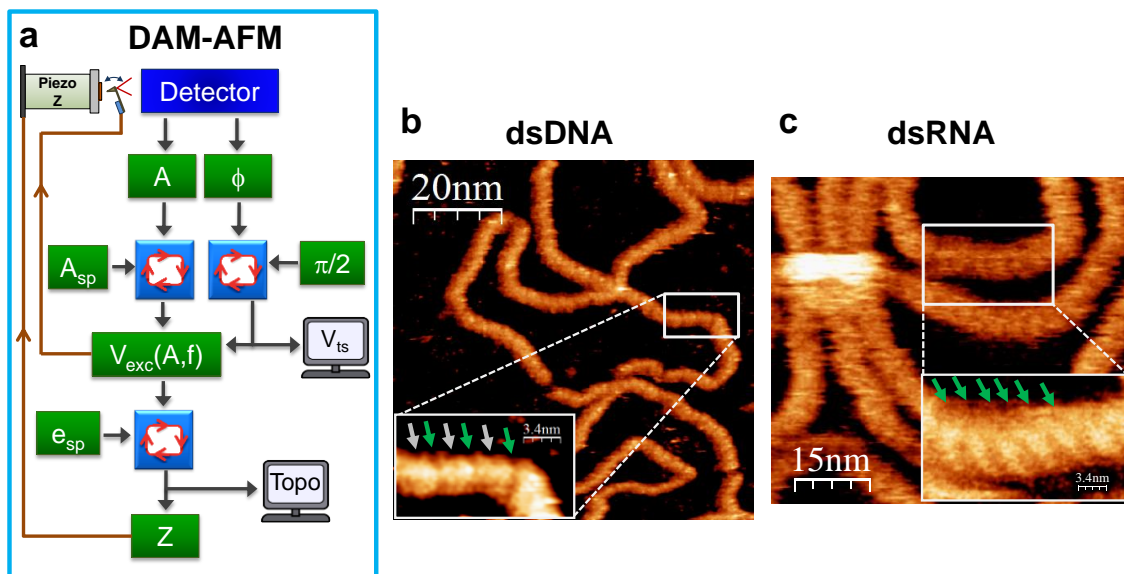


Figure 2. Drive Amplitude Modulation AFM mode and high-resolution imaging of dsDNA and dsRNA. **a)** Diagram of DAM-AFM mode experimental setup. **b)** DAM-AFM high-resolution image of dsDNA. Inset shows a fragment of dsDNA, where its major and minor grooves are resolved. **c)** DAM-AFM high-resolution image of dsRNA, where the helical periodicity was resolved (inset). Panels **a** and **c**, [3] - Adapted with permission of The Royal Society of Chemistry.

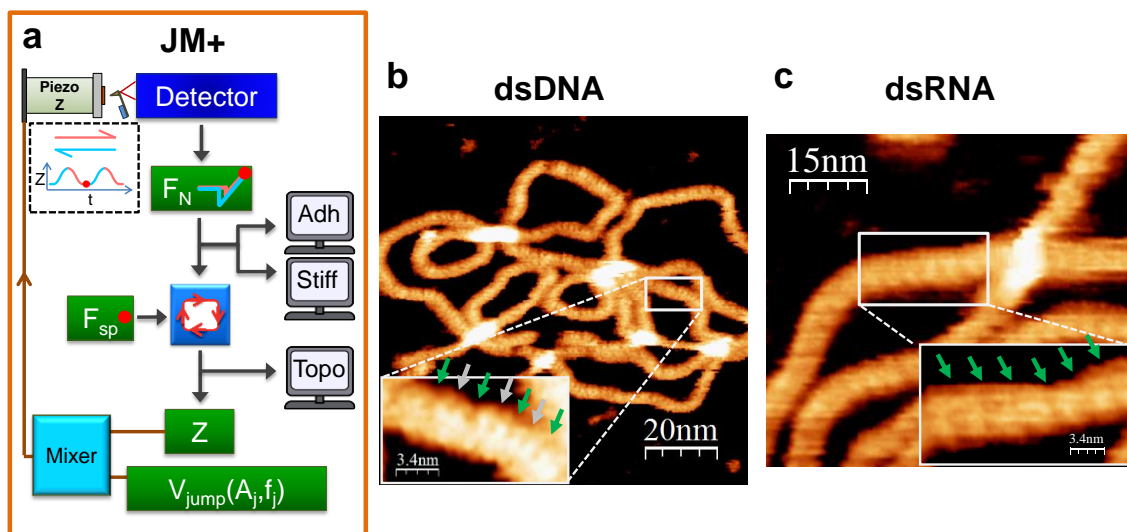


Figure 3. *Jumping Mode Plus and high-resolution imaging of dsDNA and dsRNA.* **a)** Diagram of JM+ mode experimental setup. **b)** JM+ high-resolution image of dsDNA. Inset shows a fragment of dsDNA, where its major and minor grooves are resolved. **c)** JM+ high-resolution image of dsRNA, where the helical periodicity was resolved (inset). Panels **a** and **c**, [3] - Adapted with permission of The Royal Society of Chemistry.